Energetic electron depletions in the nightside Martian upper atmosphere revisited

Jun Cui[1], Dandan Niu[2], Hao Gu[2], Xiaoshu Wu[3], Shiqi Wu[4], Haoyu Lu[4], Lihui Chai[5], and Yong Wei[5]

[1]Sun Yat-sen University
[2]Macau University of Science and Technology
[3]National Astronomical Observatories, Chinese Academy of Sciences
[4]Beihang University
[5]Institute of Geology and Geophysics, Chinese Academy of Sciences

November 23, 2022

Abstract

Energetic electron depletions are a notable feature of the nightside Martian upper atmosphere. In this study, we investigate systematically the variations of the occurrence of depletions with both internal and external conditions, using the extensive Solar Wind Electron Analyzer measurements made on board the Mars Atmosphere and Volatile Evolution. In addition to the known trends of increasing occurrence with decreasing altitude and increasing magnetic field intensity, our analysis reveals that depletions are more easily observed when the ambient magnetic fields are more horizontally inclined and under lower Solar Wind (SW) dynamic pressures. We also find that the occurrence increases with increasing atmospheric CO$_2$ density but this trend is restricted to low altitudes and within weakly magnetized regions only. These observations suggest that the formation of electron depletions is two folded: (1) Near strong crustal magnetic anomalies, closed magnetic loops preferentially form and shield the atmosphere from direct access of SW electrons, a process that is modulated by the upstream SW condition; (2) In weakly magnetized regions, SW electrons precipitate into the atmosphere unhindered but with an intensity substantially reduced at low altitudes due to inelastic collisions with ambient neutrals. In addition, our analysis reveals that both the ionospheric plasma content and thermal electron temperature are clearly reduced in regions with depletions than those without, supporting SW electron precipitation as an important source of external energy driving the variability in the deep nightside Martian upper atmosphere and ionosphere.

u

y

Corresponding author: J. Cui, cuijun7@mail.sysu.edu.cn

[illegible]

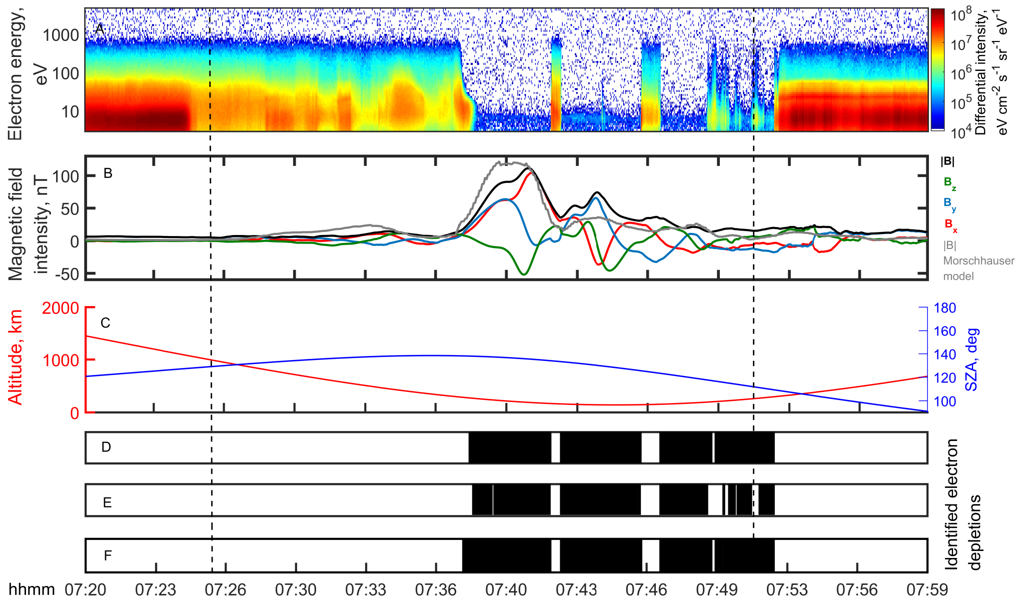

Observations of energetic electron depletions during MAVEN orbit #3416 on 1 July 2016 with a periapsis altitude of 141 km and a periapsis SZA of 128°. (A) The SWEA electron intensity from 3 eV to 4.6 keV averaged over the instrument FOV; (B) The magnetic eld intensity based on the MAG measurements along with the three components in the local coordinate; (C) The spacecraft altitude and SZA; (D)-(F) The electron depletions identi ed according to our method and those of *Steckiewicz et al.* [2015] and *Xu et al.* [2017]. The two vertical lines in the gure encompass regions within the optical shadow, where the presence of energetic electron depletions is clearly revealed by the data. The crustal magnetic eld model of *Morschhauser et al.* [2014] is superimposed in panel (B) for comparison.

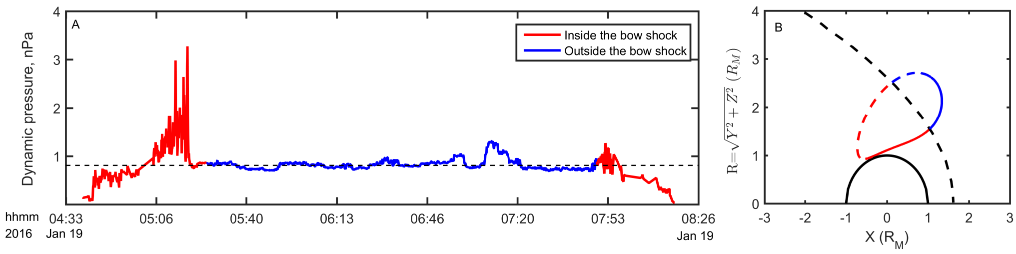

(A) The variation of dynamic pressure during MAVEN orbit #2537 on 19 January 2016, with the measurements outside and inside the bow shock indicated by blue and red, respectively. The horizontal dashed line shows the average upstream SW dynamic pressure obtained for this orbit. (B) The orbital trajectory in the MSO coordinate with the nominal bow shock location of *Trotignon et al.* [2006] given by the dashed line. R is the solid body radius of Mars.

[illegible]

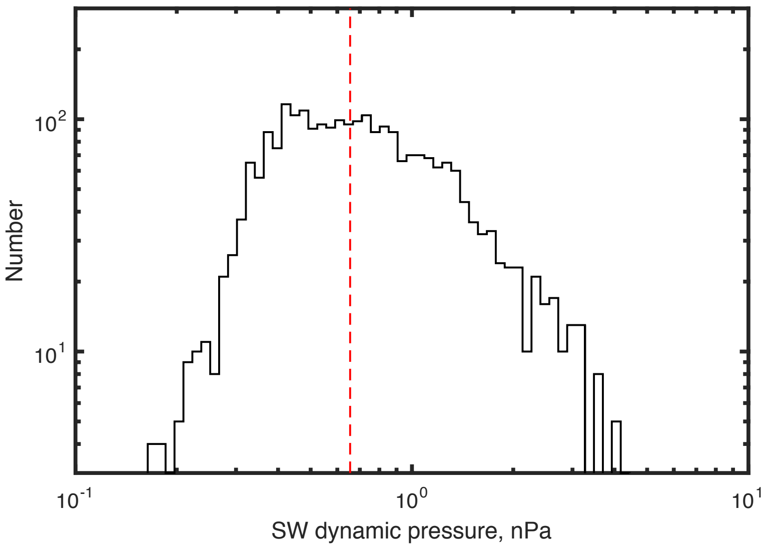

The distribution of SW dynamical pressure from all orbits included in this study, where the vertical dashed line corresponds to the median value of 0.65 nPa separating the entire data set into two subsamples with low and high SW dynamic pressures, respectively.

[illegible]

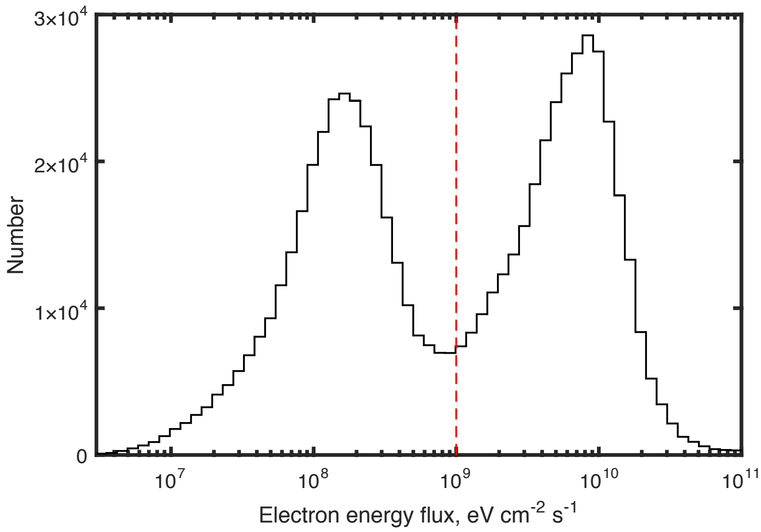

The distribution of the electron energy ux integrated over the energy range of 3 eV to 4.6 keV based on all SWEA measurements made below 500 km and within the optical shadow. The gure reveals two widely separated peaks from which a xed threshold of 1×10^9 eV cm^{-2} s^{-1}, indicated by the vertical dashed line, is used to identify electron depletions in this study.

[illegible]

[illegible]

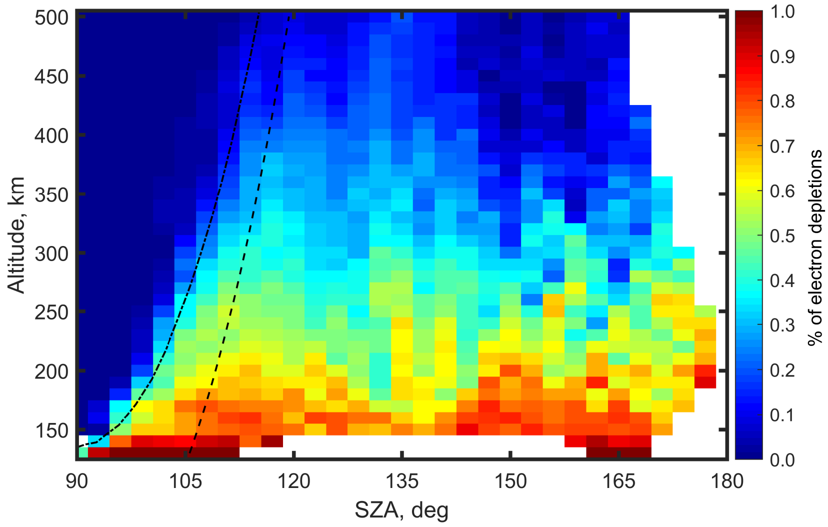

The altitude and SZA variations of the fractional occurrence of energetic electron depletions. The dashed line represents the edge of the optical shadow on Mars whereas the dash-dotted line shows the EUV terminator determined by *Lillis et al.* [2018].

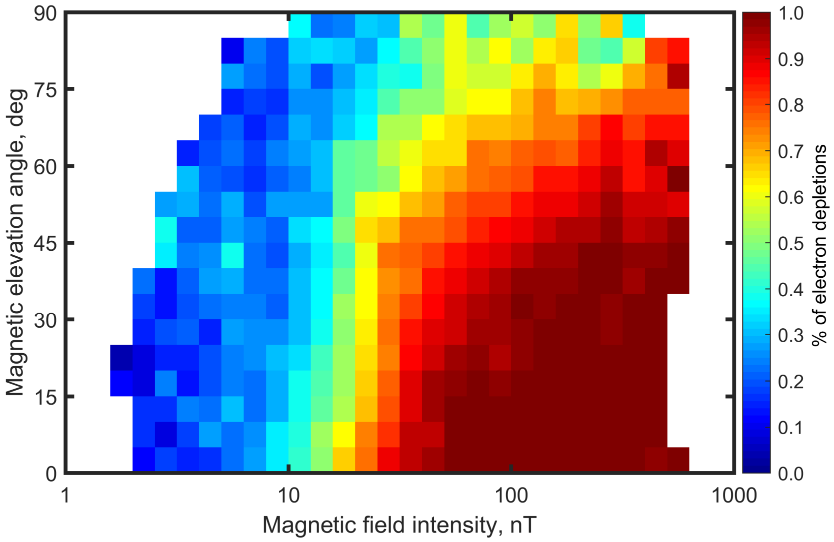

The dependence of the occurrence of electron depletions on the ambient magnetic eld con guration below 300 km and for SZA 110°.

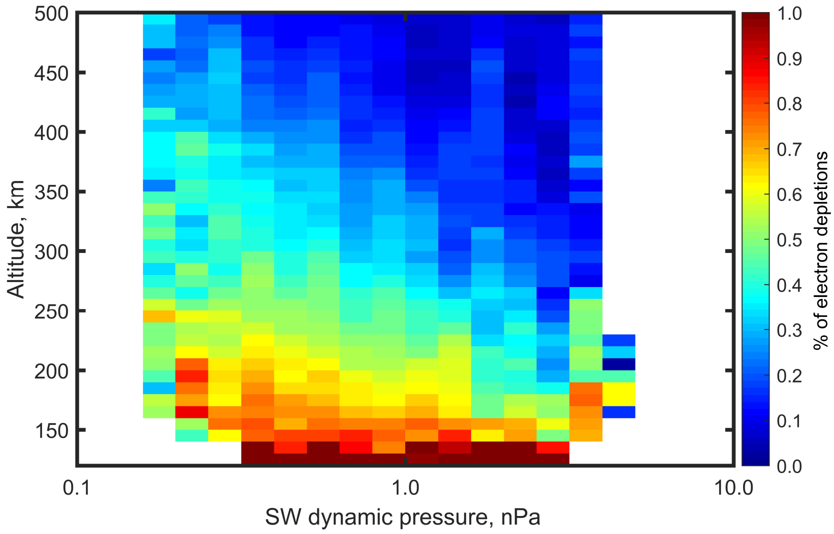

The variations of the occurrence of electron depletions with altitude and SW dynamic pressure for SZA 120°.

[illegible]

[illegible]

[illegible]

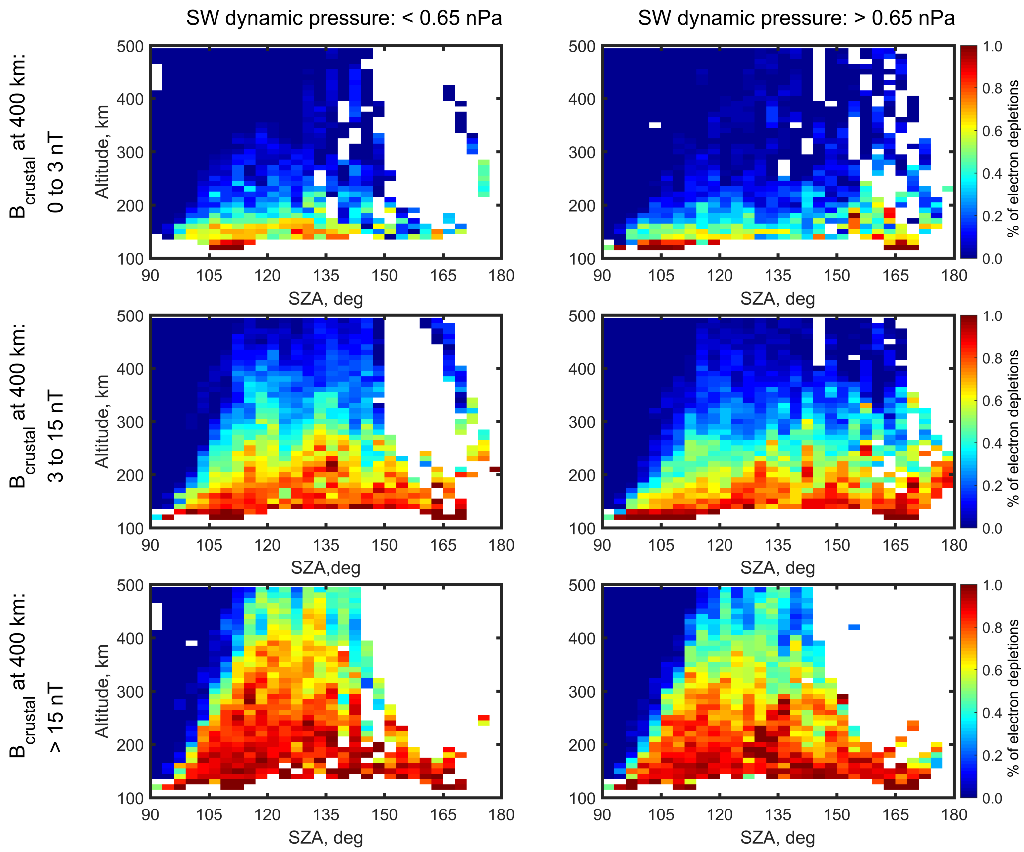

252 The variations of the occurrence of electron depletions with altitude and SZA for

253 di erent ranges of crustal magnetic eld intensity as indicated in the gure legend. The left and

254 right columns compare the situations under low and high SW dynamic pressures.

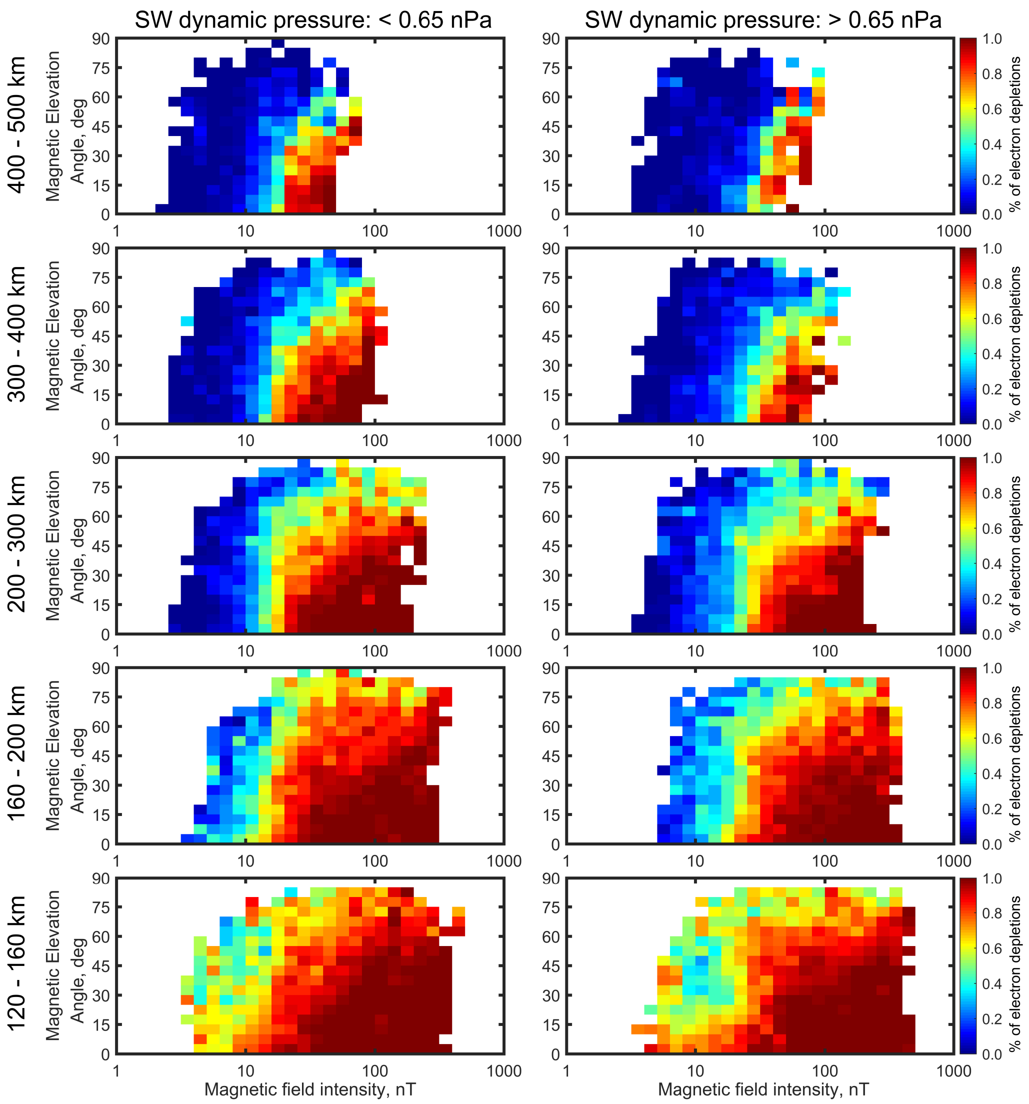

255 The variations of the occurrence of electron depletions with magnetic eld intensity
256 and elevation angle for di erent altitude ranges as indicated in the gure legend. The situa-
257 tions under low and high SW dynamic pressures are compared. Only the measurements made at
258 SZA 120° are included.

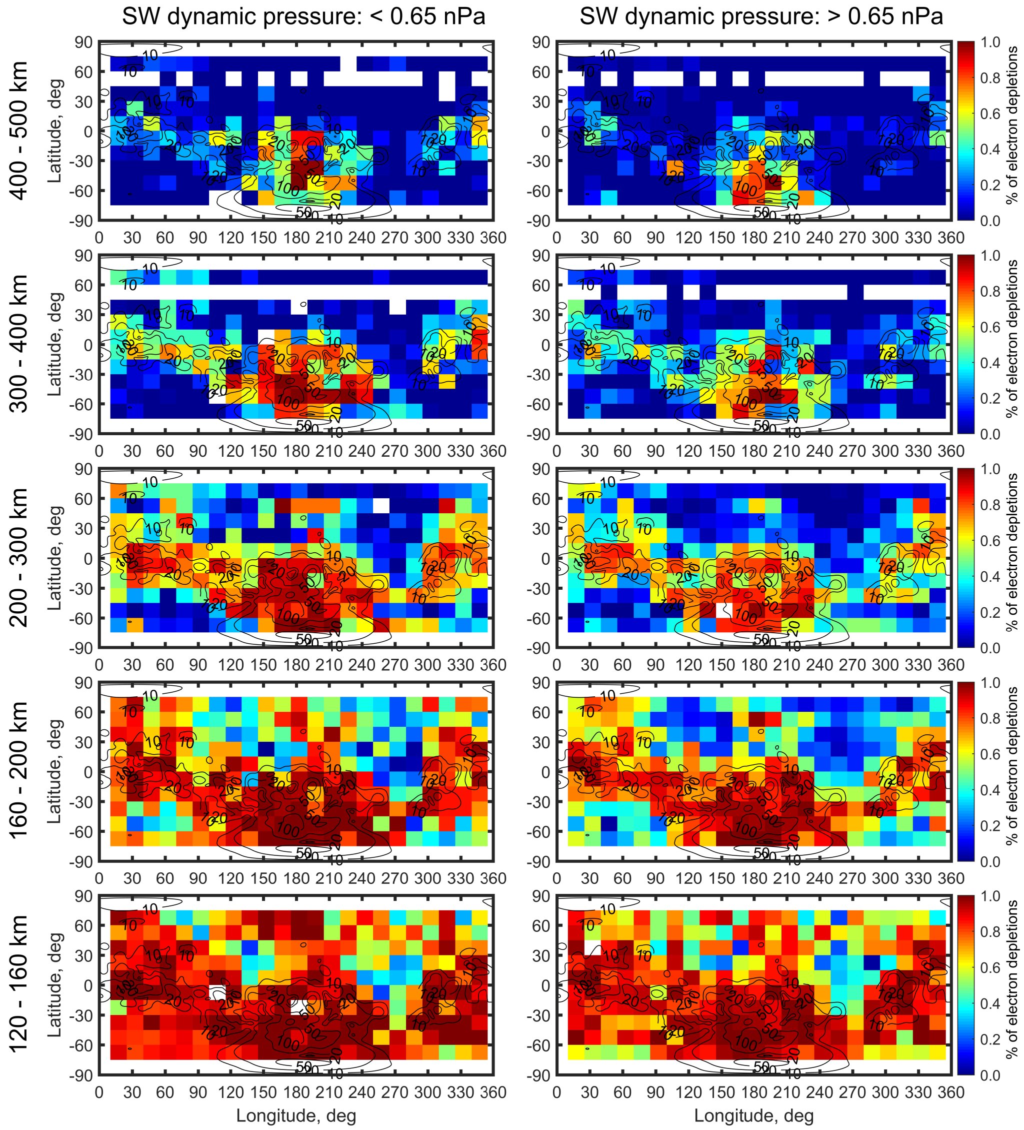

The variations of the occurrence of electron depletions with geographic longitude and latitude for di erent altitude ranges as indicated in the gure legend. The situations under low and high SW dynamic pressures are compared. Only the measurements made at SZA 120° are included. For reference, the crustal magnetic eld model of *Morschhauser et al.* [2014] at an altitude of 400 km is superimposed in each panel.

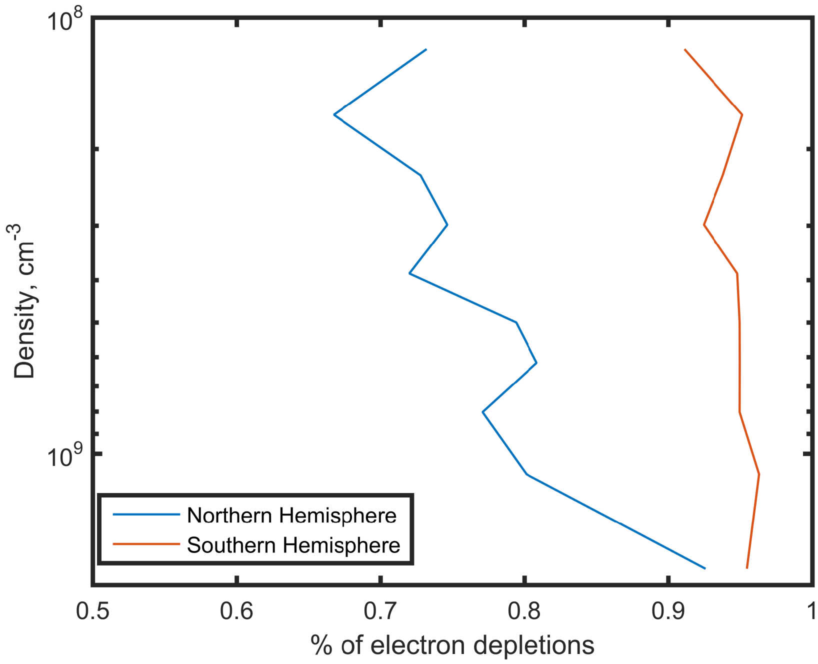

The fractional occurrence of electron depletions as a function of CO_2 density for SZA 120°, restricted to a narrow altitude range of 130-150 km. The situations for the northern and southern hemispheres are shown separately. Only the inbound data are included.

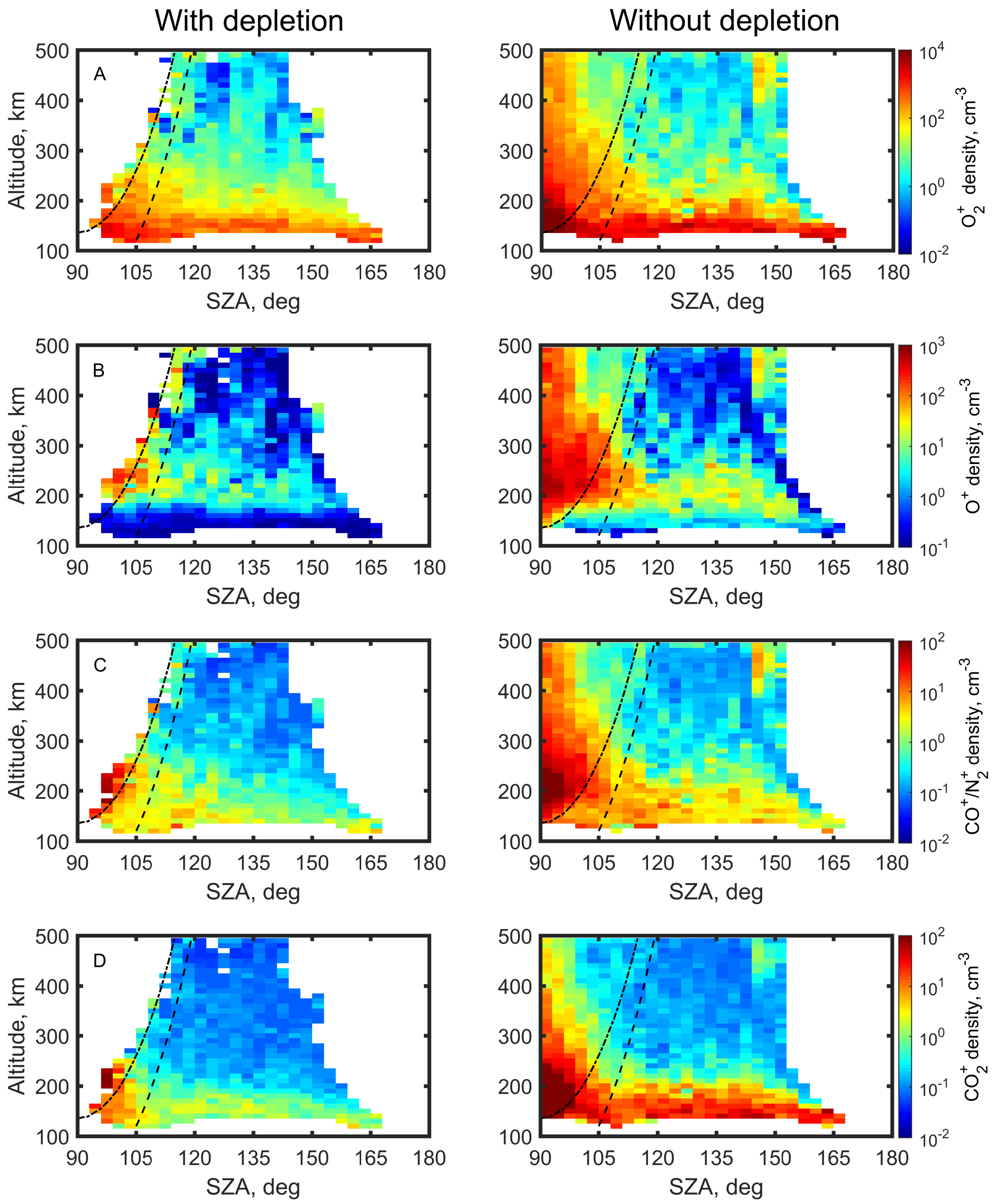

The distributions of O_2, O , CO_2, and N_2/CO in the nightside Martian ionosphere with respect to altitude and SZA, comparing the situations with and without electron depletions. In all panels, the dashed line represents the edge of the optical shadow on Mars whereas the dash-dotted line shows the EUV terminator determined by *Lillis et al.* [2018].

Figure 13. Similar to Figure 12 but for the distribution of NO^+ in the nightside Martian ionosphere.

played ion species. A similar finding was reported by Girazian et al. [2017a] who compared the nightside averaged ion density profiles under high and low incident energetic electron fluxes, both irrespective of SZA.

For regions close to the EUV terminator, the observed variations of ion densities in Figure 12 should be interpreted with caution because this is where the nightside ionosphere is more likely supported by day-to-night plasma transport rather than SW electron precipitation [e.g. Withers et al., 2012; Cui et al., 2015]. Despite this, the ion distributions between regions with and without depletions are still remarkably different, which could be interpreted by the fact that the closed magnetic loops with both footprints on the nightside should not only hinder the precipitation of SW electrons but also hinder the horizontal transport of ionospheric plasma from the dayside. This is consistent with the recent study of Cao et al. [2019] revealing that day-to-night transport in the Martian ionosphere tends to be suppressed in the presence of strong crustal magnetic fields.

A further complication is encountered for the long-lived ions which could be replenished by ion-neutral reactions during day-to-night transport [e.g. Gonzalez-Galindo et al., 2013], analogous to the situation occurring on Titan [Cui et al., 2009b]. A notable example in the nightside Martian ionosphere is NO^+ that is replenished by the reactions of O^+ and O_2^+ with atmospheric N_2 [Girazian et al., 2017b]. The density distribution of NO^+ with altitude and SZA is shown in Figure 13. The difference between regions with and without depletions appears to be substantially reduced relative to the differ-

6 Concluding remarks

[illegible]

[illegible]

Acknowledgments

[illegible]

References

[illegible]

[illegible]

the lithospheric magnetic field of Mars, Journal of Geophysical Research: Planets, 119(6), 1162–1188, doi:10.1002/2013JE004555.

Nagy, A. F., D. Winterhalter, K. Sauer, T. E. Cravens, S. Brecht, C. Mazelle, D. Crider, E. Kallio, A. Zakharov, E. Dubinin, M. Verigin, G. Kotova, W. I. Axford, C. Bertucci, and J. G. Trotignon (2004), The plasma Environment of Mars, Space Science Reviews, 111(1), 33–114, doi:10.1023/B:SPAC.0000032718.47512.92.

Ness, N. F., M. H. Acuña, J. E. P. Connerney, A. J. Kliore, T. K. Breus, A. M. Krymskii, P. Cloutier, and S. J. Bauer (2000), Effects of magnetic anomalies discovered at Mars on the structure of the Martian ionosphere and solar wind interaction as follows from radio occultation experiments, Journal of Geophysical Research, 105(A7), 15,991–16,004, doi:10.1029/1999JA000212.

Peterson, W. K., C. M. Fowler, L. A. Andersson, E. M. B. Thiemann, S. K. Jain, M. Mayyasi, T. M. Esman, R. Yelle, M. Benna, and J. Espley (2018), Martian Electron Temperatures in the Subsolar Region: MAVEN Observations Compared to a One-Dimensional Model, Journal of Geophysical Research: Space Physics, 123(7), 5960–5973, doi:10.1029/2018JA025406.

Pilinski, M., S. Bougher, K. Greer, E. Thiemann, L. Andersson, M. Benna, and M. Elrod (2018), First Evidence of Persistent Nighttime Temperature Structures in the Neutral Thermosphere of Mars, Geophysical Research Letters, 45, 8819–8825, doi:10.1029/2018GL078761.

Steckiewicz, M., C. Mazelle, P. Garnier, N. André, E. Penou, A. Beth, J. A. Sauvaud, D. Toublanc, D. L. Mitchell, J. P. McFadden, J. G. Luhmann, R. J. Lillis, J. E. P. Connerney, J. R. Espley, L. Andersson, J. S. Halekas, D. E. Larson, and B. M. Jakosky (2015), Altitude dependence of nightside Martian suprathermal electron depletions as revealed by MAVEN observations, Geophysical Research Letters, 42(21), 8877–8884, doi:10.1002/2015GL065257.

Steckiewicz, M., P. Garnier, N. André, D. L. Mitchell, L. Andersson, E. Penou, A. Beth, A. Fedorov, J. A. Sauvaud, and C. Mazelle (2017), Comparative study of the Martian suprathermal electron depletions based on Mars Global Surveyor, Mars Express, and Mars Atmosphere and Volatile EvolutioN mission observations, Journal of Geophysical Research: Space Physics, 122(1), 857–873, doi:10.1002/2016JA023205.

Steckiewicz, M., P. Garnier, R. Lillis, D. Toublanc, F. Leblanc, D. L. Mitchell,

L. Andersson, and C. Mazelle (2019), Dawn/Dusk Asymmetry of the Martian UltraViolet Terminator Observed Through Suprathermal Electron Depletions, Journal of Geophysical Research: Space Physics, 124(8), 7283–7300, doi:10.1029/2018JA026336.

Stone, S. W., R. V. Yelle, M. Benna, M. K. Elrod, and P. R. Mahaffy (2018), Thermal Structure of the Martian Upper Atmosphere From MAVEN NGIMS, Journal of Geophysical Research: Planets, 123(11), 2842–2867, doi:10.1029/2018JE005559.

Trotignon, J. G., C. Mazelle, C. Bertucci, and M. H. Acuña (2006), Martian shock and magnetic pile-up boundary positions and shapes determined from the Phobos 2 and Mars Global Surveyor data sets, Planetary and Space Science, 54(4), 357–369, doi:10.1016/j.pss.2006.01.003.

Withers, P., M. O. Fillingim, R. J. Lillis, B. Häusler, D. P. Hinson, G. L. Tyler, M. Pätzold, K. Peter, S. Tellmann, and O. Witasse (2012), Observations of the nightside ionosphere of Mars by the Mars Express Radio Science Experiment (MaRS), Journal of Geophysical Research: Space Physics, 117(A12), A12307, doi:10.1029/2012JA018185.

Wu, X. S., J. Cui, S. S. Xu, R. J. Lillis, R. V. Yelle, N. J. T. Edberg, E. Vigren, Z. J. Rong, K. Fan, J. P. Guo, Y. T. Cao, F. Y. Jiang, Y. Wei, and D. L. Mitchell (2019), The Morphology of the Topside Martian Ionosphere: Implications on Bulk Ion Flow, Journal of Geophysical Research: Planets, 124(3), 734–751, doi:10.1029/2018JE005895.

Xu, S., D. Mitchell, M. Liemohn, C. Dong, S. Bougher, M. Fillingim, R. Lillis, J. McFadden, C. Mazelle, J. Connerney, and B. Jakosky (2016), Deep nightside photoelectron observations by MAVEN SWEA: Implications for Martian northern hemispheric magnetic topology and nightside ionosphere source, Geophysical Research Letters, 43(17), 8876–8884, doi:10.1002/2016GL070527.

Xu, S., D. Mitchell, M. Liemohn, X. Fang, Y. Ma, J. Luhmann, D. Brain, M. Steckiewicz, C. Mazelle, J. Connerney, and B. Jakosky (2017), Martian low-altitude magnetic topology deduced from MAVEN/SWEA observations, Journal of Geophysical Research: Space Physics, 122(2), 1831–1852, doi:10.1002/2016JA023467.